JOURNAL OF OPTOELECTRONICS AND ADVANCED MATERIALS Vol. 8, No. 3, June 2006, p. 1216 - 1220

The correlation of morphology and surface resistance in porous silicon

SH. D. MILANI[a], R. S. DARIANI[a,b*], A. MORTEZAALI[a], V. DAADMEHR[a], K. ROBBIE[b]
[a]*Department of Physics, Alzahra University, Tehran, 19938, Iran*
[b]*Department of Physics, Queen's University, Kingston, Ontario, K7L 3N6, Canada*

We have studied the dependence of porous silicon morphology on fabrication conditions and the link between morphology, porosity and surface resistance. Porosity of the samples and thickness were determined gravimetrically. Electron microscopy reveals the evolution of porous silicon layer morphology with variation in preparation conditions. Mean size of silicon nano particles decreases with increased silicon porosity as revealed in photoluminescence spectra, I-V characteristics and surface resistance. Results are consistent with the quantum confinement model of porous silicon luminescence.

(Received April 20, 2006; accepted after revision May 25, 2006)

Keywords: Porous silicon, Surface resistance, Photoluminescence, Nano particles

1. Introduction

The efficient luminescence at room temperature in porous silicon (PS) found by Canham in 1990 provoked great interest due to its potential for optoelectronic applications. Progress in PS optoelectronics depends on understanding of the operating principles of PS device structures. However, less research has been done on the electrical transport of PS device structures compared to the study of optical properties. Several models have been proposed for the transport of carriers in PS based metal/PS/c-Si device structures [1-5], explaining experimental results assuming either that reverse current is determined by the surface transport mechanism of hopping [3], or with carrier generation in surface states at the boundary between porous silicon and the c-Si substrate [2]. It was found that the forward current-voltage (I-V) dependence exhibits a relatively short exponential region with a quality factor of 4 or higher [2-5].

In this paper, we survey optoelectronic effects in PS with experimental measurements of photoluminescence (PL), current-voltage, surface resistance, and specular reflectance of PS samples prepared with increasing etching time. We clarify the relationship between the observed behavior and porosity, and show a band-gap increase from 1.83 eV to 2 eV.

2. Experimental

The starting samples were two kinds, first n-type silicon with 1.5 Ω·cm resistivity, and second p-type silicon with 8-12 Ω·cm resistivity. The thickness of the silicon wafers was 381±15 μm and they were (111) oriented crystals. Before anodization, the wafers were cleaned with acetone and deionized water. An ohmic contact was obtained by evaporating a thin Al film onto the backside of the wafer. During anodization, this backside was covered with an acid-proof wax for protection. The PS layer was obtained by anodization in a (1:1) ethanol/HF (38%) solution at a current density of 25 mA/cm^2 for 10-50 min and then air-dried. The thickness of the PS layer was 3-7 μm.

Room temperature photoluminescence was excited with a mercury lamp (435.8 nm line). The PL emission spectrum from PS was analyzed with a set of eight bandpass optical filters with 40 nm bandwidths, and measured with a photocell and a Keithley 485 pico-ammeter. The morphology of PS samples was observed with a Philips XL30 scanning electron microscope (SEM). A Cary-500 spectrometer was used to measure scattering spectra, using a bandwidth of 1 nm. The spectra were obtained at room temperature in the wavelength range 200-3000 nm.

3. Results and discussion

Porosity of the PS samples (n-type) was determined by a gravimetric method [6] and by SEM. The variation of porosity in samples prepared with various anodization times, is presented in Table 1.

Table 1. Dependence of porous silicon (n-type) porosity on anodization time.

	Electrolytes Concentration (x:y)	Current Density (mA/cm^2)	Anodization Time (min)	Thickness (μm)	Porosity (%)
1	1:1	25	10	3.3	27
2	1:1	25	20	5.6	46
3	1:1	25	30	7.1	56
4	1:1	25	40	5.2	43
5	1:1	25	50	6.7	53

We can see that overall porosity of PS depends on anodization time, rising with anodization time and reaching roughly the saturation [7], which seems to be here t =30 min. (Fig. 1). Increasing PS porosity shrinks the size of silicon particles. Thereafter, the PS develops cracks and small pores start to grow again. There appears to be an oscillatory behavior of the etching. The thickness of the PS samples is positively correlated to porosity and anodization time (see Table 1).

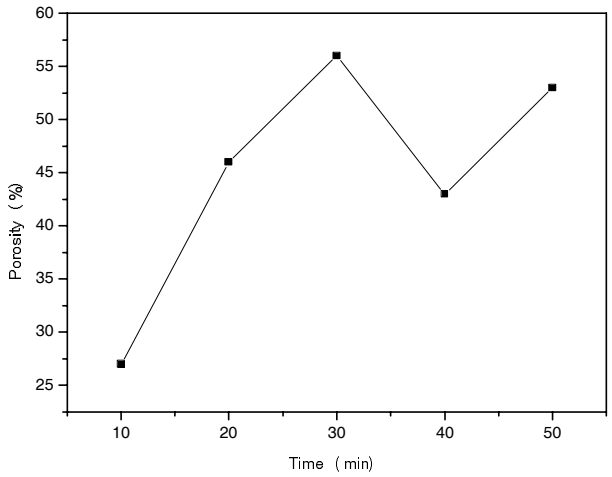

Fig.1. Porosity dependence of n-type PS samples to anodization time.

Fig. 2 shows the morphology of three samples prepared at anodization times of 20, 30 and 40 min, respectively denoted (2), (3) and (4). The electron micrograph of surface of PS sample (3) reveals its highly porous nature, while samples (2) and (4) appear to have a lower porosity. Sample (4) and (5) had an anodization time of 40 min and 50 min respectively, which is longer than the anodization saturation time of 30 min, so the pores have begun again to grow. The SEM image of (3) is presented at a higher magnification than (2) or (4) to better reveal the details of the highly porous structure. At higher magnification it becomes difficult to resolve the structure of sample (2) and (4) due to their small pore size relative to the resolution limit of the electron microscope.

Observation of pore size and morphology was obtained from SEM cross-sectional views, and results for samples (2), (3) and (4) are presented in Fig. 3. For the PS sample (3) the pores were wide and the walls partially cracked. For sample (2), prepared with shorter etching time, the pores were thinner, similar to those observed in PS sample (4).

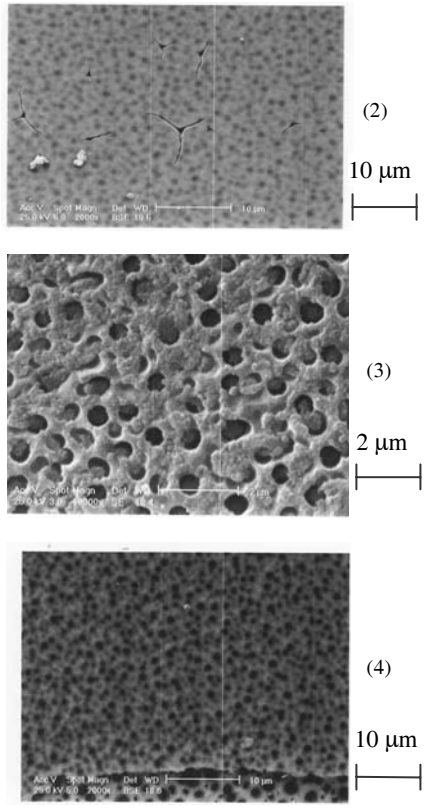

Fig. 2. Top view scanning electron micrographs of three porous silicon samples (n-type) fabricated in etching solutions with different anodization time (top) 20 min, (mid) 30 min and (bottom) 40 min.

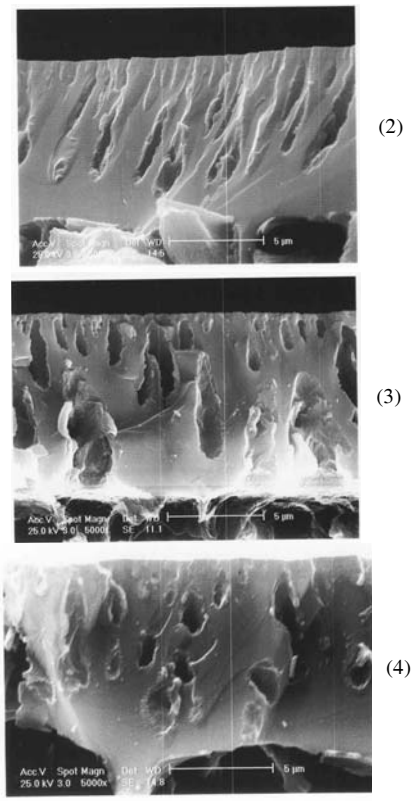

Fig. 3. Cross-sectional electron micrographs of porous films with details of pore morphology for porous silicon samples (n - type) (2), (3) and (4), top to bottom respectively.

PL spectra of the PS samples listed in Table 1 are presented in Fig. 4. We see that the PL maximum shifts to shorter wavelength with increased electrochemical anodization time. Visually, the color changes from dark golden-brown through gold to yellow as the porosity of the layer gradually increases from 27% to 56%. The PL band also becomes less intense as it shifts into the visible from the near infrared. The behavior of PL after the etching saturation time (30 min) corroborates the non-monotonic gravimetric measurements of porosity, and is again consistent with the quantum confinement mechanism: as PS porosity increases the mean size of silicon nanoparticles shrinks and the PL maximum shifts toward the blue, as we confirm here.

The observed dependence on preparation conditions, of PL emission spectra from PS, was correlated with PS surface morphology determined by SEM. PS samples prepared at the same anodization time revealed similar morphology in the electron microscope for a broad range of current densities, whereas substantial differences were observed for samples prepared at different anodization times. On the basis of the SEM images we can better understand the shift of PS luminescence maximum: PS samples prepared for the same anodization time show similar morphology for all applied current densities; the rise of overall porosity is accompanied with a relatively small blue shift of the PL maximum. On the other hand, PS samples prepared at different HF concentrations exhibit distinctly different morphology, resulting in a large blue shift of the PL maximum. Similar behavior of PL shift with porosity was reported by Dian et al. [8] who explained their observations by correlation of PL shift with PS morphology and optical properties. SEM supports our explanation of porosity PL shift behavior with a direct view of sample morphology.

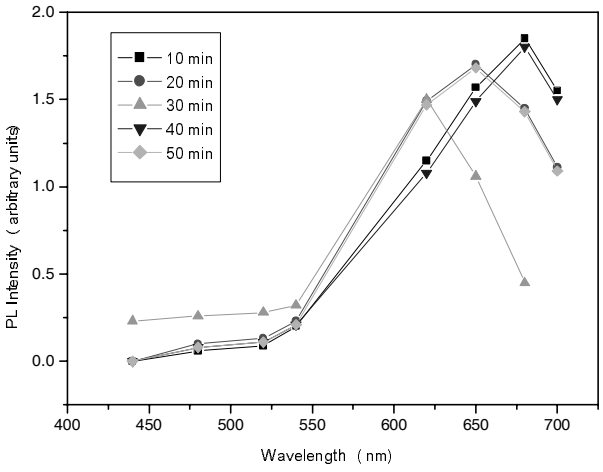

Fig. 4. Room temperature photoluminescence spectra of PS films (n-type Si) prepared at various anodization time 10 min, 20 min, 30 min, 40 min and 50 min.

We also measured electronic current-voltage (I-V) characteristics at various porosities for a Ag/PS/Si/Al sandwich structure. Samples with porosities listed in Table 1 exhibit the response curves of Fig. 5, with the c-Si curve added for comparison. Positive bias is applied to the top Al contact. All samples exhibit a rectifying junction response with turn-on voltage increasing with increasing anodization time. An exception is the behaviour for 40 min. anodization time. Increasing anodization time reduces the current for all forward biases, due to reduced mobility in the increasingly porous PS layer.

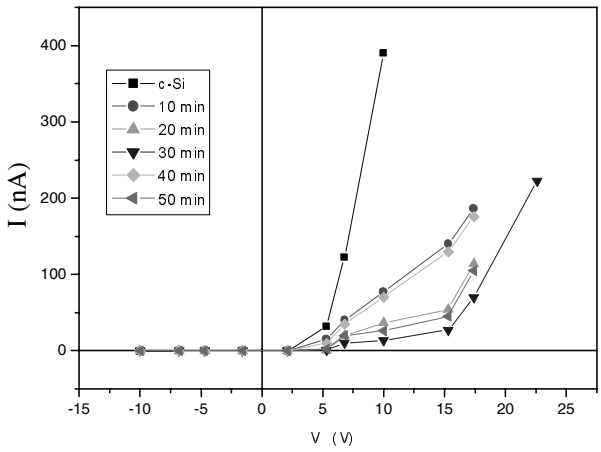

Fig. 5. I-V characteristics of a Ag/PS/Si/Al structure measured at various anodization time. For comparison we measured I-V for a c-Si wafer.

Surface resistance measurement

Measurements of surface resistance were made with the Van der Pauw method [9, 10]. Fig. 6 shows the surface resistance of PS samples of various porosities, held in the dark. With increasing anodization time (porosity), surface resistance increased up to a saturation time (t = 30 min) then decreased. Consistent with our measurements of porosity and typical size of the morphological structure, we see increasing resistance of the PS as the size of the silicon structure approaches the atomic scale. Once the PS is atomically porous, the etchant can access and dissolve the initial PS layer, and reveal the underlying (and denser) structure that then becomes available for conduction. The geometry and pore size in PS is complex, prompting for example demonstration as the adsorbing layer in a gas sensor in Barillaro et al. [11] and Gao et al. [12].

We repeated the surface resistance measurements for sample illuminated with light of varying wavelength (Fig. 7). The results show reduced resistance with increasing photon energy of the illuminating light for all samples, likely due to increased generation of electron-hole pairs. The resistance again reaches a peak with etching time (t = 30 min) then decreases, as shown in Fig. 7 and Fig. 8, with the c-Si spectrum for comparison. The similarity between the curves from 10 and 40 min, and also between 20 and 50 min etched samples suggests that the structures have similar morphological structures.

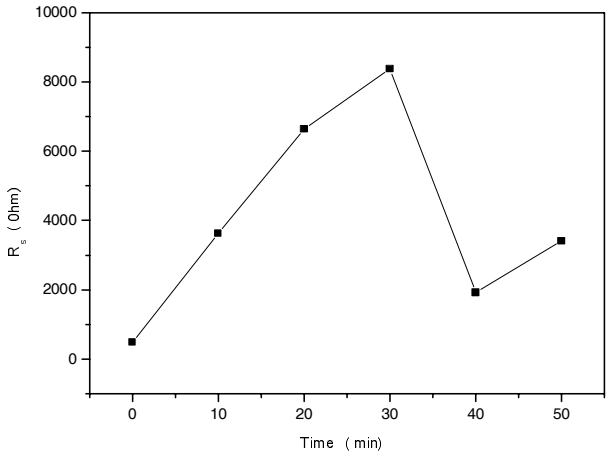

Fig. 6. Surface resistance of PS samples versus different anodization time in the dark, c-Si (t =0), 10 min, 20 min, 30 min, 40 min and 50 min.

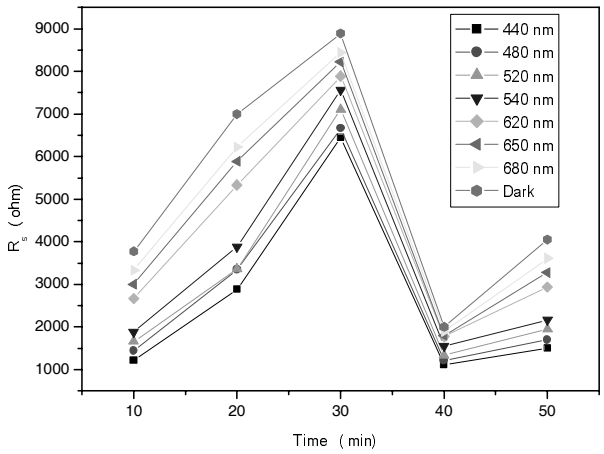

Fig. 7. Surface resistance of PS samples versus anodization time when exposed to light at different wavelengths.

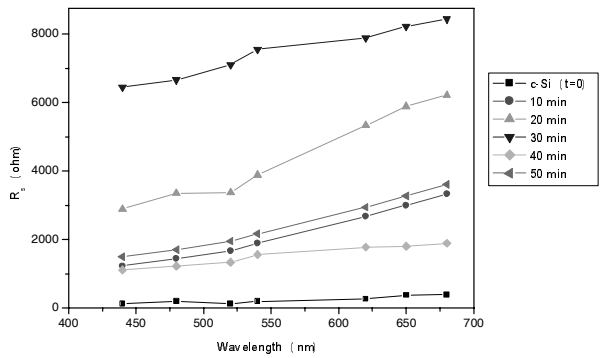

Fig. 8. Surface resistance of PS samples versus wavelength of light for different anodization times from t=0 to 50 min.

Reflectance of p-type PS Samples

We measured specular reflectance from PS sample prepared with various etching times. Our samples, made from a p-type silicon wafer, are listed in Table 2.

Table 2. Dependence of porous Si (p-type) on anodization time.

	Electrolytes Concentration (x:y)	Current Density (mA/cm^2)	Anodization Time (min)	Thickness (μm)	Porosity (%)
6	1:1	25	10	5.2	30
7	1:1	25	20	8.7	43
8	1:1	25	30	9.1	60
9	1:1	25	40	8.2	40
10	1:1	25	50	8.8	45

Fig. 9 shows the specular reflectance (%) versus light wavelength for the five PS samples. The top curve (most reflective) is c-Si while the curves below are PS prepared with increasing etch times. All curves agree with Davies-Bennett theory [13] and at long wavelengths tend to constant values. As also seen in PL and resistivity, there is a minimum in reflectivity for samples etched for 40 min, and samples etched 30 and 50 min exhibit similar response. Reduced specular reflectance is believed to be the result of increased diffuse light scattering from the morphology of the increasingly porous structure.

We measured the root means square height, or roughness, (σ) for our PS samples through Davies-Bennett theory (Fig. 10). The Fig shows σ in the range of 46 nm-87 nm as we expected. Again, σ increases with the etching time and reaches a saturation level.

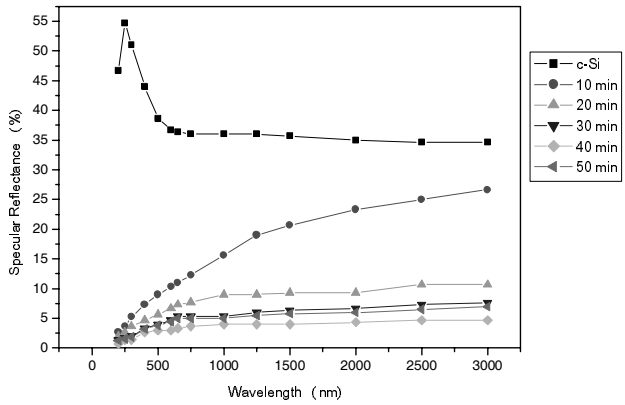

Fig. 9. Specular reflectance versus wavelength for different PS samples (formed on p-type Si).

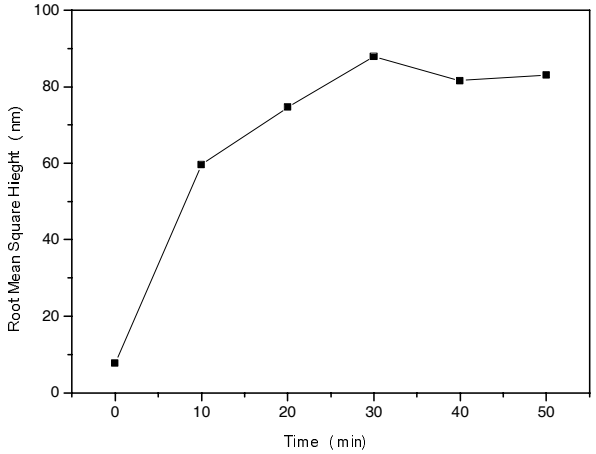

Fig. 10. Root mean square height (σ) versus anodization time.

4. Conclusion

We have found that although the total porosity of porous silicon can be determined relatively simply by a gravimetric method and electron microscopy, this parameter can only partially explain luminescence spectra and electrical current transport. An apparently cyclic variation in porosity with anodization time reveals oscillatory creation and etching of pores in silicon, with potential applications in finely controlling the atomic-scale structure in this promising optoelectronic material.

References

[1] L. A. Balagurov, D. G. Yarkin, E. A. Petrova, A. F. Orlov, S. Ya. Andrushin, J. Appl. Phys. **82**, 4647 (1997).
[2] D. B. Dimitrov, Phys. Rev. B **51**, 1562 (1995).
[3] D. Deresmes, V. Marisael, D. Stievenard, C. Ortega, Thin Solid Films. **255**, 258 (1995).
[4] Z. Chen, T. Y. Lee, G. Bosman, J. Appl. Phys. **76**, 2499 (1994).
[5] V. Yu. Timoshenko, P. K. Kashkarov, A. B. Matveeva, E. A. Konstantinova, H. Flietner, Th. Dittrich, Thin Solid Films. **276**, 216 (1996).
[6] P. Menna, G. Di Francia, V. La Ferrara, Solar Energy Materials and Solar Cells, **37**, 13 (1995).
[7] L. T. Canham, Properties of Porous Silicon, INSPEC, London (1997).
[8] J. Dian, A. Macek, D. Niznansky, I. Nemec, V. Vrkoslav, T. Chvojka, I. Jelinek, Applied Surface Science **238**, 169-174 (2004).
[9] L. J. Van der Pauw, Philips Res. Repts. **13**, 1-9 (1958).
[10] L. J. Van der Pauw, Philips Tech. Rev. **20**, 220 (1958).
[11] G. Barillaro, A. Diligenti, G. Marola, L. M. Strambini, Sensors and Actuators B in press (2004).
[12] T. Gao, J. Gao, M. J. Sailor, Langmuir **18**, 9953 (2002).
[13] G. Lerondel, R. Romestain, Thin Solid Films, **297**, 114 (1997).

*Corresponding author: dariani@physics.queensu.ca